Lawrence Berkeley National Laboratory

Title

Determination of unsaturated flow paths in a randomly distributed fracture network

Permalink

https://escholarship.org/uc/item/5jc6w621

Authors

Zhang, Keni
Wu, Yu-Shu
Bodvarsson, G.S.
et al.

Publication Date

2003-02-17

Determination of Unsaturated Flow Paths in a Randomly Distributed Fracture Network

Keni Zhang, Yu-Shu Wu, G. S. Bodvarsson, and Hui-Hai Liu

Earth Sciences Division, Lawrence Berkeley National Laboratory, University of California, 1 Cyclotron Road, Berkeley, CA 94720, PH (510)486-7393; FAX(510)486-5686; email: kzhang@lbl.gov

Abstract

We present a numerical investigation of steady flow paths in a two-dimensional, unsaturated discrete-fracture network. The fracture network is constructed using field measurement data including fracture density, trace lengths, and orientations from a particular site. The fracture network with a size of 100m×150m contains more than 20,000 fractures. The steady state unsaturated flow in the fracture network is investigated for different boundary conditions. Simulation results indicate that the flow paths are generally vertical, and horizontal fractures mainly provide pathways between neighboring vertical paths. The simulation results support that the average spacing between flow paths in a layered system tends to increase or flow becomes more focused with depth as long as flow is gravity driven (Liu et al. 2002).

Introduction

It is widely recognized that fractures play an important role in flow and transport process through unsaturated geologic strata. Because fracture permeability is often substantially greater than rock matrix permeability, fracture networks have the potential for being highly effective pathways for conducting fluid. Because of the complexity in fracture geometry and connectivity of site-specific fractured rock, flow behavior through unsaturated fractures is difficult to characterize for a given site (Bodvarsson, et al. 2002). Even with the significant progress that has been made in the past decades, flow processes in unsaturated fractured rock are currently still poorly understood. This poor understanding results mainly from technical difficulties in observing details of flow processes and accurately describing such phenomena within fractured rocks. However, flow processes occurring at this scale are of importance for many field-scale applications.

In recent years, considerable progress has been made in understanding flow processes within unsaturated fractured rocks, through field studies as well as mathematical simulations. The conventional approach for describing flow in partially saturated fractured media employs macroscale continuum concepts (Peters and Klavetteer, 1988). Those approaches use large-scale volume-averaging for homogenizing heterogeneous fracture and matrix permeabilities. Some researchers have adopted an approach to conceptualize heterogeneous fractured media with a stochastic spatial distribution of fracture permeability (Pruess, 1998; Bodvarsson, et al. 2002). Pruess (1998) proposed a continuum-based mechanistic model for investigating localized flow. In his model, water seepage under different boundary conditions in a small number of heterogeneous fractures was investigated. Bodvarsson et al. (2002) use a similar approach to

investigate the development of flow focusing and discrete-path development that may occur through unsaturated fractures within the Topopah Spring Tuff (TSw) unit of the Yucca Mountain site. To quantify flow-focusing behavior, their stochastic fracture-continuum models incorporated fracture data measured from the welded tuffs to study flow-allocation mechanisms and patterns.

In this study, we present a numerical investigation of steady flow paths in large-scale two-dimensional unsaturated fracture networks. Previous studies of flow and transport in fracture networks are limited to a small number of fractures (Kwichlis and Healy, 1993), a relatively small scale (Liu et al., 2002), or a regular pattern of fracture distributions (Therrien and Sudicky, 1996; Liu and Bodvarsson, 2001). Our model will consider more sophisticated fracture-network geometry. The fracture network in our study consists of tens of thousands of fractures, with fracture distribution in the network developed from statistical information derived from field-measured fracture data. Therefore, the current model can more realistically represent unsaturated flow behavior at field scale.

Construction of a Fracture Network

There are different ways to computationally construct a fracture network (Chilès and de Marsily, 1993). For this study, we construct two-dimensional, vertical cross-section fracture networks using fracture mapping data, including field-measured fracture density, trace lengths, and orientations. For simplicity, each fracture in the network is randomly distributed. However, generation of the fracture network is governed by statistical information derived from the field measurement data. The statistical properties of the generated fracture network should reflect the corresponding properties of fracture distribution in the study domain.

The following numerical procedure is used to construct fracture networks in this study. First, a point is randomly generated within a vertical cross section. Second, a fracture is created using the randomly generated point as the middle point of the fracture. The length of the fracture is also randomly determined from 10 groups of fractures that have different trace lengths and different probabilities of occurrence. Orientation of the fracture is determined in the same way as its length. Orientation and trace length are considered to be independent in generating the fracture network. At the same time, the fracture aperture is computed as a function of its trace length. Third, iterations of the above two steps are performed to achieve a desired fracture density. If the study domain consists of multiple layers, this procedure needs to be repeated to generate fracture network for all layers.

Discrete fracture models are developed here to incorporate fracture data measured from the welded tuffs of the Yucca Mountain site, specifically from the bottom of the Paintbrush nonwelded (PTn) unit (a unit immediately above the TSw) to the potential repository horizon. In this study, a fracture network with a size of 100m×150m is generated to represent the highly fractured TSw unit, including subunits TSw31, TSw32, TSw33, TSw34, and TSw35. The five subunits from TSw31 to TSw35 have a thickness of 2.0, 40.0, 65.0, 38.0, and 5.0 m, respectively (Figure 1). The lengths and orientations of generated fractures are consistent with statistics of the data of 15,290 fractures, collected from detailed line surveys in underground tunnels for these

units. Table 1 shows the lengths for different fracture groups and their corresponding percentage (portion) for different units. Note that fractures with trace lengths smaller than 0.23 m were not considered in this study. Small fractures with trace lengths shorter than this cutoff may contribute little to fluid flow in the fracture network and therefore are ignored here. In addition, only a limit of number of fracture data for TSw35 unit is available. The percentage for different trace lengths for that unit presented in the table may have a large degree of uncertainty.

Table 1. Fracture length and percentage (portion) used for generating fracture networks

Group #	TSw31		TSw32		TSw33		TSw34		TSw35	
	Length (m)	Percent (%)	Length (m)	Percent (%)	Length (m)	Percent (%)	Length (m)	Percent (%)	Length (m)	Percent (%)
1	0.5	31.86	0.7	22.71	0.5	23.29	0.7	26.72	1.2	15.79
2	0.7	11.99	1.5	31.39	0.8	18.51	1.2	18.62	1.6	18.42
3	0.9	13.88	2.5	16.02	1.5	25.22	1.7	19.20	2.0	15.79
4	1.1	10.73	3.5	8.77	2.5	11.58	2.5	17.75	2.6	5.26
5	1.3	7.57	4.5	7.82	3.5	7.99	3.5	8.27	3.5	7.89
6	1.5	4.73	6.0	6.31	5.0	6.75	4.5	3.90	4.5	5.26
7	2.0	10.09	8.5	3.30	7.0	2.41	5.5	2.16	5.5	7.89
8	3.0	5.05	11.5	1.04	10.0	1.10	7.0	1.80	7.5	7.89
9	5.0	3.79	14.5	1.13	15.0	1.31	10.0	0.94	15.0	10.53
10	9.5	0.32	18.0	1.51	23.0	1.72	15.0	0.62	20.0	5.26

Fracture density is an important parameter in determining a fracture network. Measured line densities for the five units are 2.2, 1.1, 0.81, 4.3, and 3.2, respectively. The line density reflects the average number of fractures along a surveying line. We use the measured line density to generate two-dimensional fracture networks selecting different random seed, and find, in many cases, no globally connected flow path from top to bottom. Because a fracture network is three-dimensional in reality, using measured fracture line density to generate fracture network in two dimensions may lead to a lower connectivity than the real fracture system. In this study, the two-dimensional model is in fact a three-dimensional model with a unit thickness. In this case, fracture area density is instead used for generating the network. Fracture area density is defined as the number of fractures crossed to a unit area in the horizontal direction. The field measured fracture line density can be converted to area density through a numerical scheme.

Fracture area density is determined by counting the number of fractures per unit of horizontal area. The horizontal fracture network is generated assuming that the network has the same line density, trace length distribution, and orientation as its corresponding two-dimensional cross-section, which are provided by field measurement data. We construct a fracture network with 1 m in width and 100 m in length for each geological unit. The area density is obtained by dividing the total number of fractures of the network by 100. The computed area densities for TSw31 to TSw35 are 4.55, 1.6, 1.37, 6.67, and 4.08, respectively.

Based on the fracture area densities and fracture statistical information of these units, we generate a randomly distributed fracture network (Figure 1). The fracture network consists of 20,707 fractures, in which 303 fractures connect to the top boundary. About 28% of the fractures do not have a connection to the fracture system that is connected to top infiltration sources. These fractures may make a limit of contribution to the flow system. In this study, the unconnected or isolated fractures have not been included in the model.
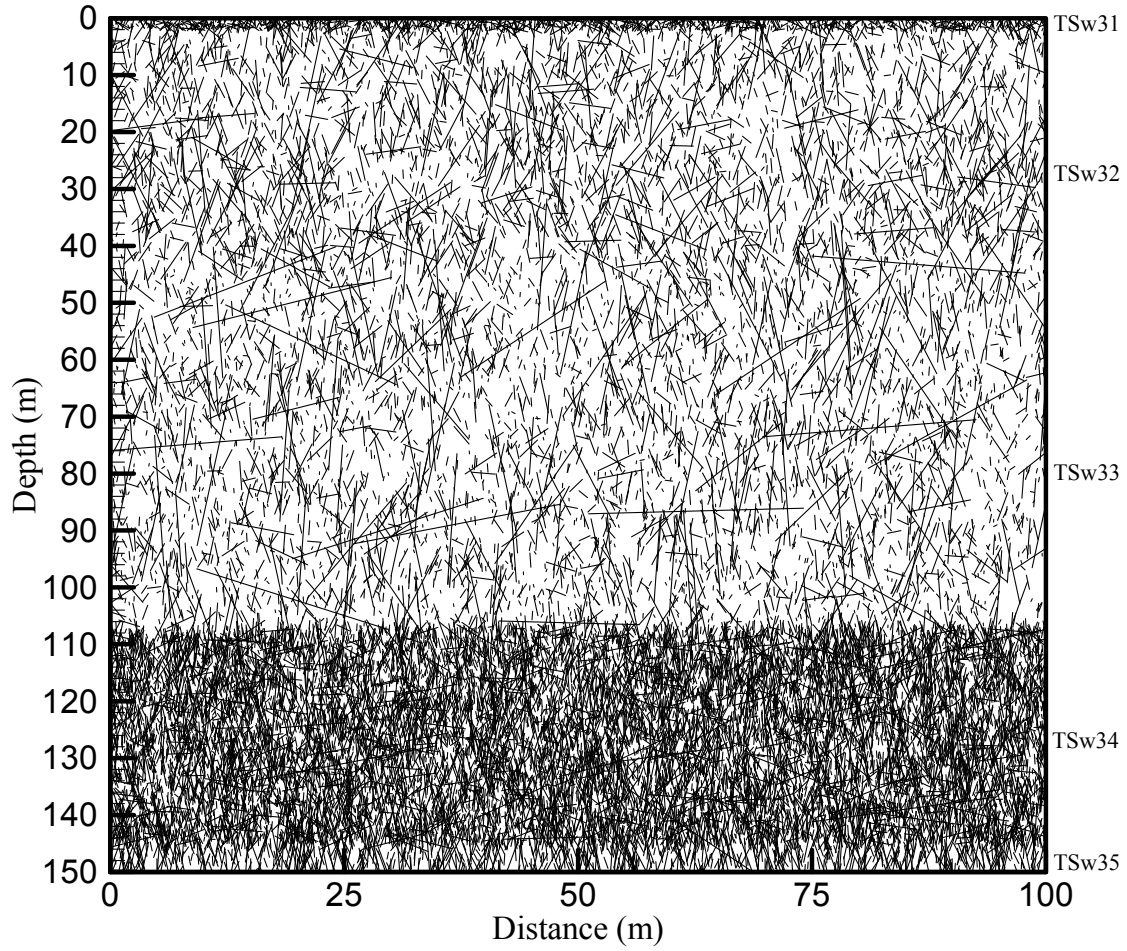
Figure 1. A fracture network generated based on statistical information derived from the field measured fracture data.

Fracture aperture is another important geometric parameter for fracture flow, which determines the permeability of a parallel-plate fracture (de Marsily, 1986). It was found that the thickness of a fracture filled with calcite or another material is strongly positively corrected with its trace length (Chilès and de Marsily, 1993]. In this study, we follow the equation provided by Liu and Bodvarsson (2001) to determine fracture aperture:

$$b = cL^d \tag{1}$$

where b is the fracture average aperture, L is its trace length, and c and d are empirical constants. Based on air-permeability and fracture-density data from the TSw unit, Liu and Bodvarsson (2001) estimated the constants c and d to be 1.008×10^{-4} and 0.317, respectively. We use these two constants and the trace length of the 10 groups of fractures to determine their corresponding average fracture aperture.

4

Flow Simulation

The fracture network is discretized into 126,432 linear elements. The linear elements have a maximum length of 1m. The intersection point of any two fractures is treated as an element. Volume of these intersection elements can be extremely small. Therefore, the volumes of the fracture elements may differ by several orders of magnitude.

Previous theoretical and experimental work suggests that relative permeability and capillary pressure behavior of fractures is similar to that of highly permeable media with intergranular porosity (e.g. Pruess and Tsang, 1990; Persoff and Pruess, 1995). As a result, the constitutive relationships of the van Genuchten (1980) model are selected (Liu and Bodvarsson (2001) have provided a detail of discussion of this issue). Input parameters for fractures include fracture permeability, van Genuchten α and m parameters, porosity, and interface area. We adopt the same scheme as discussed by Liu and Bodvarsson (2001) for computing fracture permeability and the van Genuchten α parameter. The parameter m is an index of aperture size distribution for an individual fracture and is given a value of 0.633 in this study. The residual saturation S_r and the satiated saturation S_s, which will be used in the van Genuchten model, are assigned values of 0.01 and 1, respectively.

The flow simulations are carried out by introducing water at various time-independent rates into the top of the fracture network (shown in Figure 2). Because of the strong heterogeneities and complex fracture connections present in fractures along the top boundary, it is impossible to simply distribute desired infiltration water uniformly over all fractures crossing the top boundary. We accomplish infiltration by attaching an additional gridblock to the top of the fracture network. The entire top boundary of the network is connected to this single block and a prescribed infiltration rate is applied to it. As water is injected into this block, water eventually flows into the fractures beneath the block. This outflow will in general partition non-uniformly among the fractures. After a rapid initial transient, this infiltration block will reach a steady flow condition. Thus, a constant infiltration rate will apply to the top boundary of the network. Infiltration applies only to the fractures along the top boundary. Side boundaries are considered impermeable, and a free drainage condition is imposed at the bottom boundary.

The steady-state unsaturated water flow through the fracture network system is simulated using TOUGH2_MP code (Zhang et al., 2001), a parallel version of TOUGH2 code (Pruess, 1991). Because randomly distributed fractures can lead to an extremely complex element connection system, and because elements may have large differences in volume, numerical modeling difficulties can arise, requiring intensive computational effort. We found that it is necessary to use more efficient numerical methods to perform the simulations; specially, one of the solutions we used is to introduce parallel computing techniques for the simulations. All computations are conducted using 64 processors on an IBM SP RS/6000 supercomputer. Previous study has shown that the TOUGH2_MP may achieve a linear speedup or even super linear speedup (Wu et al., 2002). In addition, we also use the constant-volume approach to improve simulation convergence rate. It is clear that the volume of elements does not affect the final, steady-state solutions. Consequently, constant volume for all elements is used in our simulation. The constant-volume approach can dramatically speed up the simulation.
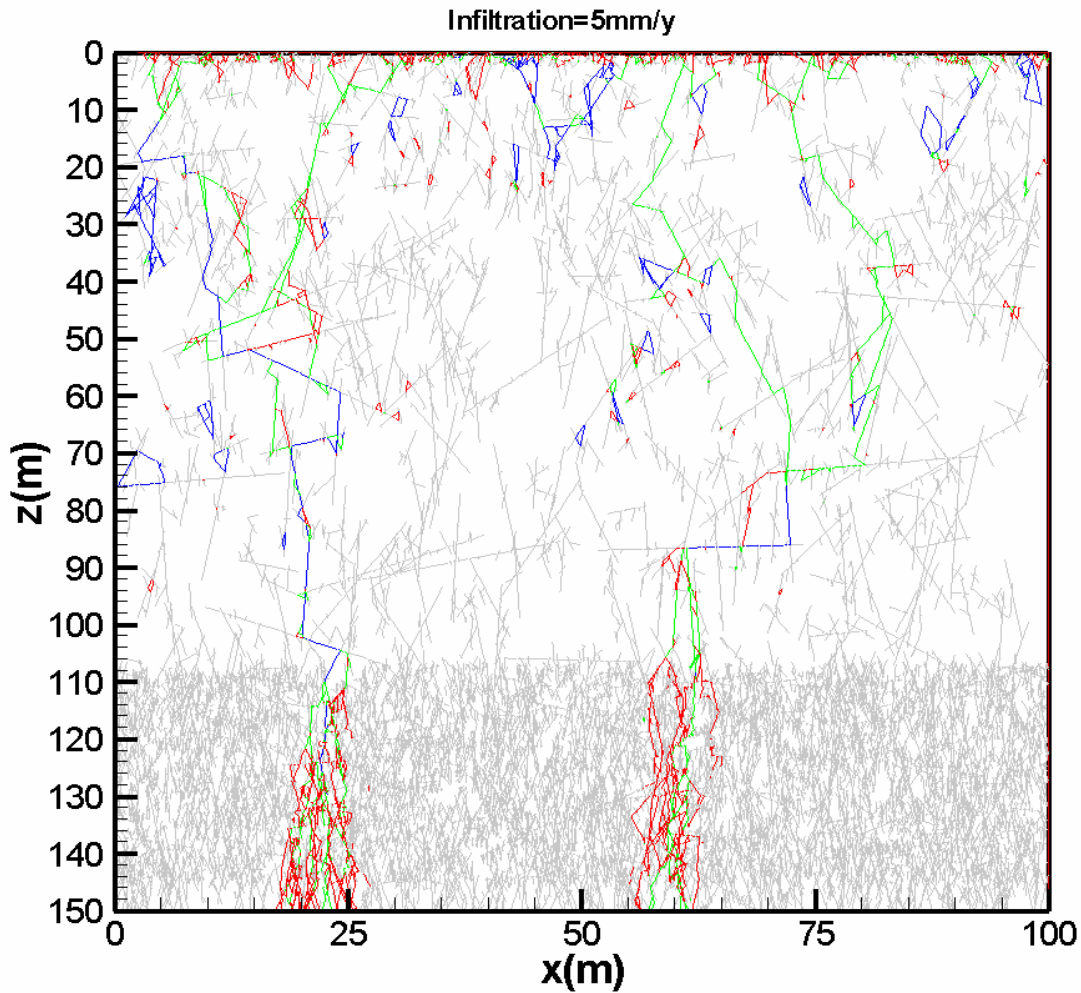
Figure 2. Simulated steady state flux distribution in the fracture network, q=5mm/year (Flux magnitude is represented in four different colors in decreasing sequence of blue, green, red and grey. Each color represents one-order-of- magnitude difference in flux).

Simulation Results and Analysis

A total of three simulation cases are run with different infiltration rates applied to the top of the fracture network. The three schemes are designed to test the influence of different infiltration rates on flow paths. Flow paths are determined by the water flux magnitude presented in four different colors including blue, green, red and grey. Each color represents one-order-of-magnitude difference in flux. For example, the blue color represents the highest water flux, about three orders higher than the grey one. We use the same color scheme for all simulation results.

Figure 2, 3, and 4 show flow paths within the unsaturated fracture network for infiltration rate of 5 mm/y, 50 mm/y, and 500 mm/y respectively. The flow generally proceeds in vertical fractures. At the upper part, several flow paths, developed from top infiltration, either merge or remain separate as water continues to migrate downward. Clearly, there are only two main flow paths developed in these cases. The three cases have an almost identical flow pattern, except for differences in flux magnitude and the spreading range in TSw34 and TSw35 unit. Higher

6

infiltration rate on the top boundary leads to a larger spreading range of the flow paths in these units. We can conclude that the influence of top infiltration rates on the flow pattern is not significant.
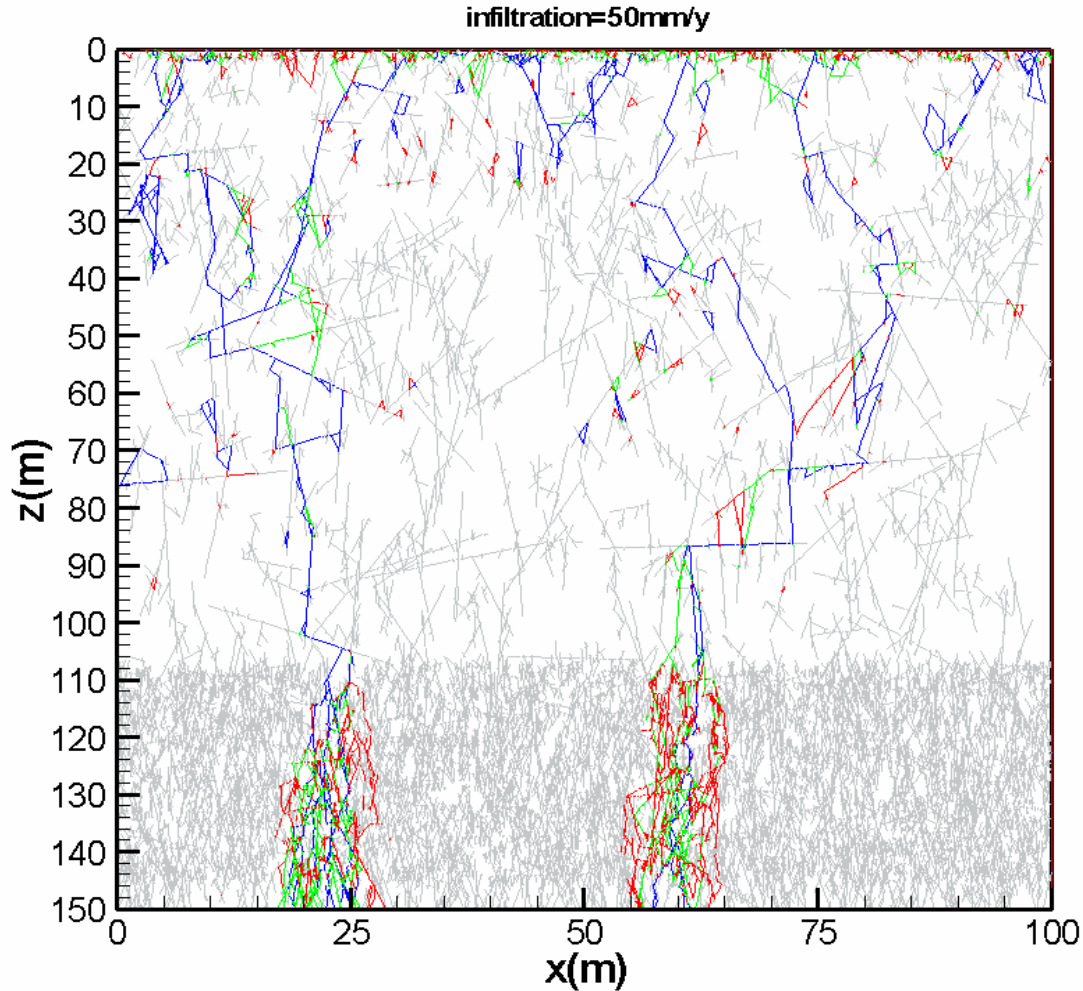

Figure 3. Simulated steady state flux distribution in the fracture network, q=50mm/year (Flux magnitude is represented in four different colors in decreasing sequence of blue, green, red and grey. Each color represents one-order-of- magnitude difference in flux).

Flow paths are controlled mainly by connected fractures. From the fracture network, we find that at least four connected paths exist from top to bottom. However, not all connected paths can develop into flow paths. In the upper part of the unsaturated fracture work, the flow paths consist primarily of fractures that have relatively long trace lengths. Similar phenomena have been reported by Liu et al. (2002). In this upper part, the fractures have a relatively lower density. However, this phenomenon may not exist for a higher-density fracture network. In the lower part of the fracture network, the long and short fractures have similar contributions to the development of flow paths. This finding is consistent with the study of de Dreuzy et al. (2001)

that the connectivity of a fracture network is a function of fracture density and fracture length range. When fracture density is high, the contribution of fracture length to the network connectivity lessens. Fracture-network connectivity is one of the most important parameters determining flow path development, only connected fractures developing into a flow path.
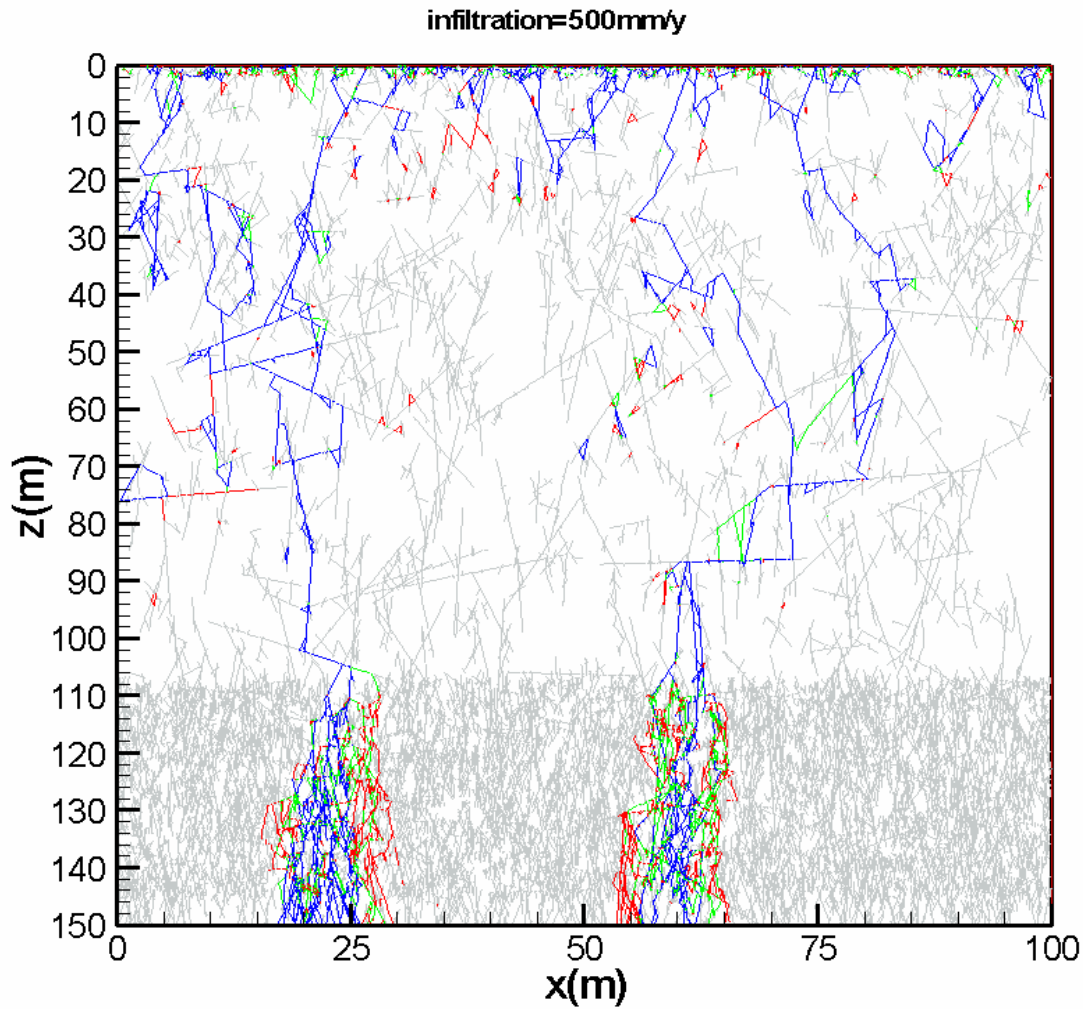

Figure 4. Simulated steady state flux distribution in the fracture network, q=500mm/year (Flux magnitude is represented in four different colors in decreasing sequence of blue, green, red and grey. Each color represents one-order-of- magnitude difference in flux).

Flow patterns of the simulation results confirm the hypothesis of Liu et al. (2002) that average spacing between paths in a layered system tends to increase with depth as long as flow is gravity-driven. They gave a synthetic example of a geological medium consisting of three layers involving a downward unsaturated flow process. In that fracture network, both the top and bottom layer have 10 connected vertical fractures, with the middle layer having two. Because of the limitation of connected fracture numbers at the middle layer, Liu et al. (2002) believe only two flow paths can be developed in the bottom layer, even though there are 10 vertically

8

connected paths in that layer. Our simulation results have demonstrated a similar conclusion. In Tsw31 unit, there are about several tens flow paths. The flow paths reduce to less than 10 in Tsw32 and two in Tsw33. Tsw34 has very high fracture density and more connected paths. However, owing to the limitation of flow paths in Tsw33, only two flow paths develop in Tsw34. Since vertical water flow has a certain degree of horizon dispersion, each flow path at the bottom of Tsw34 unit spreads over a range of 10 to 20 m.   The simulation results of this study thus tend to further confirm that flow path development in a layered unsaturated fracture network is depth-dependent, as long as gravity is the dominant driving force of the flow.

Summary and Conclusions

Numerical studies have been conducted to investigate the development of discrete-fracture flow paths in a two dimensional large-scale, discrete-fracture network. This paper presents a methodology for how to construct a discrete-fracture network using randomly generating fractures conditioned by statistical information generated from field measurement data. We constructed the two-dimensional fracture network based on measurement data of fracture density, length range, and distribution directions. Each fracture in the network is randomly distributed. The statistical properties of generated fracture networks should reflect the corresponding properties of fracture distribution in the study domain.

The modeling results demonstrate that focused flow paths through fractures are generally vertical. Horizontal fractures mainly function as pathways between neighboring vertical fractures. Our results suggest that the average spacing between flow paths in a layered system tends to increase with depth (or flow becomes more focused downwards) as long as flow is gravity-driven. In addition, flow paths are found to consist primarily of long trace fractures in lower fracture-density domains. In higher fracture-density domains, long and short trace fractures both contribute to the development of flow paths.

Acknowledgments

References

Bodvarsson, G.S., Wu, Y.S., and Zhang, K. (2002). "Development of discrete flow paths in unsaturated fractures." accepted by *J. Contaminant hydrology*.

Chilès, J.P., and de Marsily, G. (1993). "Stochastic Modeling of fracture systems and their use in flow and transport modeling." In J. Bear, C.F. Tsang and G. de Marsily (eds.), *Flow and Contaminant Transport in Fractured Rock,* San Diego, California: Academic Press.

De Dreuzy, J.R., Davy, P., Bour O. (2001). "Hydraulic properties of two-dimensional random fracture networks following a power law length distribution 1. Effective connective." *water Resour. Res.*, 37(8): 2065-2078.

de Marsily, G. (1986). *Quantitative Hydrogeology*, Academic Press, San Diego, CA.

Kwicklis, E.M., and Healey, R. W. (1993). "Numerical investigation of steady liquid water flow in a variably saturated fracture network." *water Resour. Res.*, 29(12), 4091-4102.

Liu, H.H., and Bodvarsson G.S. (2001). "Constitutive relations for unsaturated flow in a fracture network." *Journal of Hydrology*, 252, 116-125.

Liu, H.H., Bodvarsson G.S., and Finsterle, S. (2002). "A note on unsaturated flow in two-dimensional fracture networks." *Water Resour. Res.*, 38(9), 1176-1184, 2002.

Persoff, P., Pruess, K. (1995). "Two-phase flow visualization and relative permeability measurement in natural rough-wall rock fractures." *Water Resur. Res.*, 31(5), 1175-1186.

Peters, R.R., Klavetter, E.A. (1988). "A continuum model for water movement in an unsaturated rock mass." *Water Resour. Res.*, 24(3), 416-430.

Pruess, K. (1991). *TOUGH2 – A general-purpose numerical simulator for multiphase fluid and heart flow*. Report LBNL-29400, Lawrence Berkeley National Laboratory, Berkeley, California.

Pruess, K. (1998). "On water seepage and fast preferential flow in heterogeneous, unsaturated rock fractures." *J. Contaminant hydrology*, 30, 333-362.

Pruess, K., and Tsang, Y.W. (1990). "On two-phase relative permeability and capillary pressure of rough-walled rock fractures." *Water Resour. Res.*, 26(9), 1915-1926.

Therrien, R., and Sudicky E.A. (1996). "Three-dimensional analysis of variably-saturated flow and solute transport in discrete-fractured porous media." *J. Contaminant hydrology*, 23, 1-44.

van Genuchten, M. Th. (1980). "A closed-form equation for predicting the hydraulic conductivity of unsaturated soils." *Soil Sci. Soc. Amer. J,* 44(5): 892-898.

Wu, Y.S., Haukwa C., and Bodvarsson G.S. (1999). "A site-scale model for fluid and heat flow in the unsaturated zone of Yucca Mountain, Nevada." *J. Contaminant hydrology*, 38(1-3): 185-217.

Wu, Y.S., Zhang, K., Ding, C., Pruess, E., Elmroth, E., and Bodvarsson, G.S. (2002). "An efficient parallel-computing method for modeling nonisothermal multiphase flow and multicomponent transport in porous and fractured media." *Advances in Water Resources*, 25, 243-261.

Zhang, K., Wu, Y.S., Ding, C., Pruess, K., and Elmroth, E. (2001). "Parallel computing techniques for large-scale reservoir simulation of multicomponent and multiphase fluid flow." Paper SPE 66343, *Proceedings of the 2001 SPE Reservoir Simulation Symposium*, Houston, Texas.